Engineering Journal issn: 0125-8281

Article

Machine Learning for Water Level Prediction in the Chao Phraya River Basin

Wilmat D.S.M. Priyasiri[1,a], Areeya Rittima[1,b,*], Jidapa Kraisangka[2], Wudhichart Sawangphol[2], Yutthana Phankamolsil[3], and Yutthana Talaluxmana[4]

1 Graduate Program in Environmental and Water Resources Engineering, Department of Civil and Environmental Engineering, Faculty of Engineering, Mahidol University, Thailand
2 Faculty of Information and Communication Technology, Mahidol University, Thailand
3 Environmental Engineering and Disaster Management Program, Mahidol University, Kanchanaburi Campus, Thailand
4 Department of Water Resources Engineering, Faculty of Engineering, Kasetsart University, Thailand
E–mail: [a]sineth.priyasiri@gmail.com, [b,*]areeya.rit@mahidol.ac.th (Corresponding author)

Abstract. High precision of hydrological prediction is crucial for real–time operation of flood and drought risk mitigation and strategic planning. This study assessed the predictive performances of three machine learning algorithms; Extreme Gradient Boosting (XGBoost), Random Forest (RF), and Deep Neural Networks (DNNs) for water level prediction. Accordingly, the one–day and one–week water level prediction models for six key gauged stations along the Chao Phraya River and its major tributaries were developed. Selecting input features was carried out based on the physical river–reservoir system using past water level, rainfall, controlled reservoir outflow, and upstream discharges with different travel times. The statistical evaluation indicated that both XGBoost and RF with rainfall input robustly outperformed than DNNs, as it strongly achieved higher R^2 from 0.937 to 0.999 for model training and from 0.743 to 0.995 for model testing and lower MAE, MSE, and RMSE values for all daily prediction scenarios. Among these algorithms, RF demonstrated the superior performance for low water level prediction exhibiting the smallest percentage error of overestimating lying between +0.0088% and +0.9380%. XGBoost, RF, and DNNs algorithms exhibited small average percentage errors for high water level prediction ranging from –2.2696% to +1.1587%. Additionally, daily model can capture the entire testing dataset with high precision than weekly model. Daily predictions provide valuable real–time insights for forecasting water levels during critical flood and drought periods. In contrast, weekly predictions assist in strategic water resource planning to address challenges in diverse hydrological environments.

Keywords: Extreme gradient boosting, random forest, deep neural networks, machine learning, artificial intelligence, water level prediction, Chao Phraya River Basin.

ENGINEERING JOURNAL Volume 29 Issue 8
Received 22 February 2025
Accepted 20 August 2025
Published 31 August 2025
Online at https://engj.org/
DOI:10.4186/ej.2025.29.8.147

DOI:10.4186/ej.2025.29.8.147

1. Introduction

High precision hydrological prediction plays a crucial role for water resource planning and management as well as disaster mitigation in the context of climate variability caused by natural and human–induced factors [1]. Hydrological prediction is a primary process in water resource management to predict the future behavior and likelihood of hydrological data in the water resources system such as rainfall, runoff, river water level, reservoir inflow, reservoir water level, etc. During normal operation, it has been adopted for water resource planning to bridge the imbalance between water availability and water requirement and establish the proper water allocation plan. During critical water situation, hydrological prediction has been served as the key supportive tool to provide key critical data and deliver informed decision to dam operators for disaster warning and mitigation like severe floods and prolonged droughts [2]. Highly precise river water level prediction is vital for practical applications like flood warning systems, real–time control of hydraulic structures [3], and drought mitigation efforts. This is because it can signal rapid floods, indicate significant river level drawdown, and monitor riverbank stability, which is affected by water level fluctuation [4] and its impact on geotechnical properties [5, 6]. Predicting the changes in river water levels commonly involves both natural and human–induced factors such as rainfall, runoff, regulated flow, watershed and meteorological conditions [7]. These factors contribute to the observable water level data exhibiting non–stationarity, non–linearity, randomness, and periodic patterns [8].

Traditionally, the physically–based modelling which is the process driven approach, has been widely applied for water level prediction. However, in–depth analysis of the physically–based modelling between watershed characteristics and hydrological processes occurred in the watershed system has demanded the numerous input data and extensive knowledge and skill of the modelers to handle the uncertainties of parameter estimation and complexity of model structures [1]. Consequently, data driven approach using statistical or Machine Learning (ML) techniques has been widely adopted for river level prediction by establishing the relationship between the input and output variables while comprehensive physical watershed characteristics are not incorporated [9–11]. Therefore, ML has been regarded as more efficient tool than the physically–based model in term of computational effort and cost [12]. Moreover, ML has produced remarkable advances in streamflow prediction providing better predictive performance than the calibrated conceptual and physical–based hydrological models [13].

For over a decade, ML has been increasingly adopted as an alternative tool in data–driven modelling across various engineering domains [14], such as product classification [15], battery sales forecasting [16], air traffic [17], structural design and analysis [18, 19], geotechnical engineering [20] and hydrological modelling [21, 22]. It has gradually substituted the traditional statistically–stochastic techniques like autoregressive and Box–Jenkins models due to drawback of computational complexity and its limited applicability to non–linear systems [10, 23]. Moreover, the fundamental stationary assumption of the statistically–stochastic models indicating constant statistical properties of hydrological data over time might not be entirely realistic for real world water scenarios. Consequently, the enhanced capability of ML for hydrological prediction has been proven and presented though many case studies worldwide [21, 22]. Moreover, ML can produce better predictive results for large scale applications when dealing with large dataset with high dimensionality and non–linearity relationship [12, 24, 25].

Several classical ML algorithms have been employed for hydrological prediction such as, linear and logistic regression, Support Vector Machines (SVM), K–Nearest Neighbors (KNN), Multi–layer Perceptron (MLP), Random Forest (RF), Gradient Boosting (GB), Extreme Gradient Boosting (XGBoost), and Radial Bias Function (RBF), etc. The recent revolution and achievement of Deep Neural Networks (DNNs) which incorporate multiple layers of artificial neural networks (ANNs), has been renowned due to ability to learn complex patterns and representations from huge datasets.

Numerous case studies worldwide have demonstrated the improved predictability and performances of various ML algorithms in hydrological applications. For example, improvement of river flow prediction by ML methods has ensured proficiency of Multi–Layer Artificial Neural Networks (ANNs) in precisely capturing the stage–discharge relation [26]. Enhanced predictive performance of maximum flood depth in the river using advanced convolutional neural networks was also exhibited [27]. The predictability of Long Short–Term Memory (LSTM) algorithm in predicting rainfall–runoff during extreme hydrological events was investigated and compared to the conceptual and process–based models [28]. Two ML algorithms; Radial Basis Function (RBF) and Support Vector Model (SVM) were developed to predict daily, weekly and monthly reservoir evaporation losses and high accuracy level of daily model with SVM was accordingly found [29]. In addition, SVM algorithm substantially outperformed in predicting daily reservoir water level than ANFIS model [7]. Three ML algorithms including Multi–Layer Perceptron Neural Network (MLP–NN), Long–Short Term Memory Neural Network (LSTM), and Extreme Gradient Boosting (XGBoost) applied for the river water level prediction were explored with the different input scenarios. These three ML prediction models showed the robust performances while MLP–NN, which is fully connected NN model with more than one layer exhibits the best predictive results for river water level prediction [10].

ML models with SVM and Gene Expression Programming (GEP) and model trees (MT) algorithms were applied to predict three standardized streamflow indices, namely Standardized Precipitation Index (SPI), Standardized Streamflow Index (SSI), and Standardized Precipitation Evapotranspiration Index (SPEI) for hydrological drought monitoring. The results showed the high precision of SPI when modelling by ML algorithms and MT could perform well in predicting SSI [30]. The application of ML algorithms focusing on drought index prediction was also implemented for drought monitoring in semi–arid region. Four significant ML algorithm including Random Forest (RF), Voting Regression, AdBoost Regressor, and K–Nearest Neighbor Regressor, were adopted to predict 1–, 3–, 9–, and 12–month SPI and SPEI drought indices. The result revealed the good predictability of these four ML algorithms in predicting 3–, and 12–month SPEI index [31].

There were research studies proven that tree–based ML algorithms such as Random Forest (RF), Gradient Boosting (GB), and Extreme Gradient Boosting (XGBoost) are more reliable than traditional and conventional ML algorithms such as Artificial Neural Network (ANN) and Radial Bias Function (RBF) for reservoir water level prediction [32]. Extreme Gradient Boosting (XGBoost) presents high level of accuracy in capturing fluctuation of river water level [33], reservoir water level [32], and also groundwater level [34]. Moreover, XGBoost is considered as operative algorithm in handling with complex and non–linear parameters that massively utilized to various ML prediction challenges [23]. It exhibits superior speediness to learn large–scale dataset and use regularization technique to prevent overfitting [23]. This algorithm can achieve the desirable results significantly faster than the traditional solutions on a single machine potentially up to ten times [27]. Importantly, XGBoost can capture sudden fluctuation in a short time of prediction data [34].

It is emphasized that optimum hyperparameter of some conventional ML algorithms strongly influences the predictive performances. Consequently, optimization algorithms can be incorporated to enhance the superiority of ML algorithms [35]. Both gradient–based optimization; gradient descent, stochastic gradient descent, and adam, and population–based optimization; Genetic Algorithm (GA), Particle Swarm Optimization (PSO), and Differential Evolution (DE), have been broadly used to tune ML hyperparameters. For example, Particle Swarm Optimization (PSO) was utilized to optimize the LSTM hyperparameter to enhance capability to learn data characteristic for water level prediction [36]. It is revealed that the better performance of the hourly short–term streamflow prediction across the spatial scale in the river basin by convolutional neural network (CNN) was substantially improved when Imperialist Competitive Algorithm (ICA) and Grey Wolf Optimizer (GWO) was incorporated to adjust the hyperparameter of CNN [37].

To enhance the predictability for hydrological prediction, hybrid prediction models integrating ML algorithms with statistical techniques both in the pre–processing (data preparation) and post–processing (prediction refinement) steps, have been implemented. For instance, the boundary–corrected maximal overlap discrete wavelet transforms (BC–MODWT) which is the signal processing technique to decompose the signal data, was deployed with DNNs for real–time rainfall and runoff prediction [38]. The monthly long–term streamflow prediction was developed by proposing the hybrid SVR–ANN combined with Bayesian Model Averaging (BMA) method in the post–processing step to refine the predictive results [39]. In addition, LSTM and Light Gradient Bossing Machine (LightGBM) integrated with reciprocal error method was developed for annual runoff prediction. The results obtained by integrated prediction model (LSTM–LightGBM) showed better performance metrics than two single prediction models (LSTM and LightGBM) [40]. Moreover, the Stacked Heterogeneous Ensemble Method (SHEM) which is an ensemble machine learning technique that combines predictions from diverse models to generate a conclusive prediction in improving the overall predictive performances, was used for rainfall prediction [41].

Due to its importance, this study employed three powerful ML algorithms; XGBoost, RF, and DNNs to predict one–day and one–week ahead water levels along the Chao Phraya River (CPYR) and its tributaries where headwater of the river flow of CPYR originates. CPYR is a principal artery located in the Chao Phraya River Basin (CPYRB) in Central Thailand. It plays a vital role in shaping history, culture, and economic development of the country. It originates in the north where four main tributaries; Ping, Wang, Yom, and Nan, join. It travels over 370 kilometers southward, eventually discharging into the Gulf of Thailand [42]. CPYR serves as a lifeline for millions of people providing water mainly for agriculture, industry, domestic use, and ecology. The river flow and water level of CPYR are significantly governed by the flow regulation of four main storage dams, namely, Bhumibol (BB), Sirikit (SK), Khwae Noi Bumrungdan (KNB) and Pasak Cholasite (PS) dams which varies seasonally due to downstream water demands and local and regional tropical climate factors. It is revealed that the annual average rainfall in the upper basin substantially ranges from 1,173 mm to 1,748 mm, exceeding annual rainfall in the lower basin which is approximately 1,100 mm [43]. The increased river flow and water levels along CPYR during monsoon season (May.–Oct.) have led to flooding particularly in inundated low–lying area downstream of Chao Phraya Diversion Dam (CPY). Conversely, during dry season (Nov.–Apr.), the decreased river flow and water level drawdown have caused the water scarcity in the lower basin. Therefore, to monitor flooding and drought situations along CPYR, six key gauged flow stations located upstream and downstream of CPY dam as shown in Fig. 1, were selected to predict water level by ML algorithms. The core novelty of this work lies in the unique and valuable dataset and the selection of key input features. These were used to establish various water level prediction models for both daily and weekly scenarios, which provide insights for real–time operation and strategic water resources planning. Furthermore, the predictive performance of these models was evaluated by exploring their capability in predicting both low and high water levels. These resulting findings contribute to improved flood and drought monitoring and control in the central region of Thailand.

2. Material and Methods

2.1. Input Features for Water Level Prediction Modelling

To develop the daily and weekly models for water level prediction, the long–term historical water level and discharge records of six gauged stations; P.17, W.4A, N.67, C.2, USCPY, and C.29, were accordingly collected to encompass various climatic conditions occurred in the region. Additionally, a wide range of potential variables such as weather parameters including rainfall, controlled outflow by upper reservoirs, and upstream discharges were collected and identified as influential factors on water levels corresponding to their statistical correlation and physical characteristic relation. To characterize the local weather influencing seasonal changes of river water level, the rainfall data for each gauged station was downloaded based on its location from the National Aeronautics and Space Administration (NASA) power product [44]. To determine proper lag time of input features in the prediction models, the travel time of upstream discharges and regulated reservoir outflow to reach the downstream gauged stations was accordingly considered. It is recognized that the significance of data correlation and feature importance increases with larger sample sizes. Consequently, the observation dataset used in this study comprised available data up to 2023 as summarized in Table 1.

After the data collection, a quality control process to ensure the data reliability was then implemented to detect minor percentage of data errors including missing values, inconsistencies, and outliers for subsequent analysis. The data entry errors in datasets were removed and missing values in between days were imputed using mean method. For extended periods of missing values, such as a week or a month or more, historical data from similar water years (dry year, normal year, and wet year) were replaced to maintain temporal relationships in datasets. Duplicate records from inconsistent datasets were detected and removed to prevent overrepresentation. The extreme outliers were preserved if representing true extreme events. However, if outliers due to technical fault were found, removal or mean methods were adopted to handle those values.

This cleaned data stored in a structured format was statistically preprocessed through correlation analysis to create appropriate input features for water level prediction by three different ML algorithms including XGBoost, RF, and DNNs. Input variables exhibiting strong statistical correlations with the target water level data were designed as potential inputs at specific gauged stations. Specifically, features demonstrating the highest correlation coefficients were prioritized during the input feature selection process in correspondence with physical interaction. Accordingly, three daily prediction scenarios, namely Scenario 1 (S1), Scenario 2 (S2), and Scenario 3 (S3), varying the prediction algorithms were designed to predict one–day ahead water levels. The objective was to test and compare their predictive performances of each scenario particularly to facilitate real–time control of hydraulic structures in the lower basin during normal and extreme conditions. Furthermore, one weekly prediction scenario, Scenario 4 (S4) using XGBoost was also developed to predict one–week ahead water levels aiming to support water management and operation planning. Selecting input features for the daily water level prediction models significantly depends on the strong relationship between two variables, while identifying the lag time of each input is determined by the travel time of water from upstream to the given gauged stations. As the weekly prediction model involves coarser data granularity of input and output variables, considering weekly averages of the river water level and relevant upstream discharge, and summed weekly values of controlled outflow and rainfall, this operation helps to smooth out short–term noise and focus on longer–term trends. Consequently, the input features for weekly water level prediction models were kept as same as daily model by ignoring lag–time interpretation. The selected input features for different scenarios of water level prediction models are summarized in Table 2. The analysis of correlation coefficient between target water level at all gauged stations and these features using daily full dataset is presented in Table 3.

It is demonstrated that target water levels are strongly correlated with their past water levels for all gauged stations with correlation coefficient of 0.856–0.998. Consequently, past water levels were identified as key inputs in water level prediction models for all gauged stations. A low correlation between rainfall and river water level data across all stations was exhibited, varying from 0.121 to 0.230. However, rainfall data collected at the same location as the target water levels was specified as a substantial input for prediction models. The results of correlation analysis for all gauged stations demonstrated mild to strong correlation between upstream discharges and target water levels at specific stations which vary from 0.266 to 0.937. Although the relation between reservoir outflows and downstream water levels varied from weak to moderate relation, with correlation coefficients of 0.045 to 0.444, these reservoir outflows were included in the water level prediction models due to physical interactions.

To predict the water level at Station P.17 at time t+1 or one–day/one–week ahead prediction, past water level at time t, rainfall at time t, reservoir outflow from the BB dam with lag time t–1, and upstream discharges with lag time t–1 at Station W.4A were specified as input features. Measuring streamflow at Station P.17 signals the water level fluctuation for flood monitoring in the CPYRB where headflow from the Ping and Wang rivers are converged. For Station W.4A measuring streamflow across the Wang river, past water level at time t and rainfall at time t were only used as input features for water level prediction at time t+1. As Station N.67 is located downstream of the SK and KNB dams measuring flow and water levels across Nan river where Yom and Nan rivers join, therefore, the input features are past water level and rainfall at time t, reservoir outflows from both SK and KNB dams with lag time t–4 and t–1, respectively, and upstream discharges from Station Y.17 at time t and Station N.22A at time t–1. Station C.2 is regarded as key crucial gauged station used for flood and drought monitoring along CPYR where head flow from four main tributaries are combined. Consequently, identifying the input features for water level prediction of Station C.2 include reservoir outflows from three main dams with different lag times; BB dam with lag time t–2, SK dam with lag time t–4, and KNB dam with lag time t–1. In addition, upper discharges from three main stations at time t; P.17, Y.17, and N.67 together with past water level and rainfall at time t were used accordingly for C.2 prediction. The precise prediction of upstream water level of CPY dam is very important for downstream flood control along the lower CPYR, therefore, predicting USCPY's water level is determined by the head flow at Station C.2, past water level and rainfall at time t. To predict water level of Station C.29, located downstream of CPY dam where PS river joins, input features include reservoir outflow from PS dam, USCPY's water level, past water level at C.29, and rainfall at time t.

The next step involved splitting the dataset into two separate sets: training set and testing set. In this study, initial 80% of the chronologically contiguous dataset was designated as the training set. This portion was used to train the model by teaching it the underlying patterns and relationships between the input features and the corresponding water levels. The final 20% of the chronologically contiguous dataset was set aside as the testing set to evaluate the performance of the trained model. The number of testing samples varied from 647 to 2,155 for all daily model scenarios and from 93 to 308 for the weekly model scenario depending on data availability of input features of each station. This testing set served as a proxy for unseen data, enabling an assessment of how well the model generalizes to new observations. In general, various methods can be employed to perform the train–test data splits, such as random sampling or time–based splitting. Since this dataset was time series data, consequently, time–based splitting was employed for train–test data splits in this study. An 80:20 train–test ratio, a widely adopted practice in machine learning, was used for all prediction scenarios. This ratio ensures that the 80% training data is substantial enough for robust parameter estimation, while the 20% testing data is sufficient to reliably assess the model's predictability and generalization capabilities.

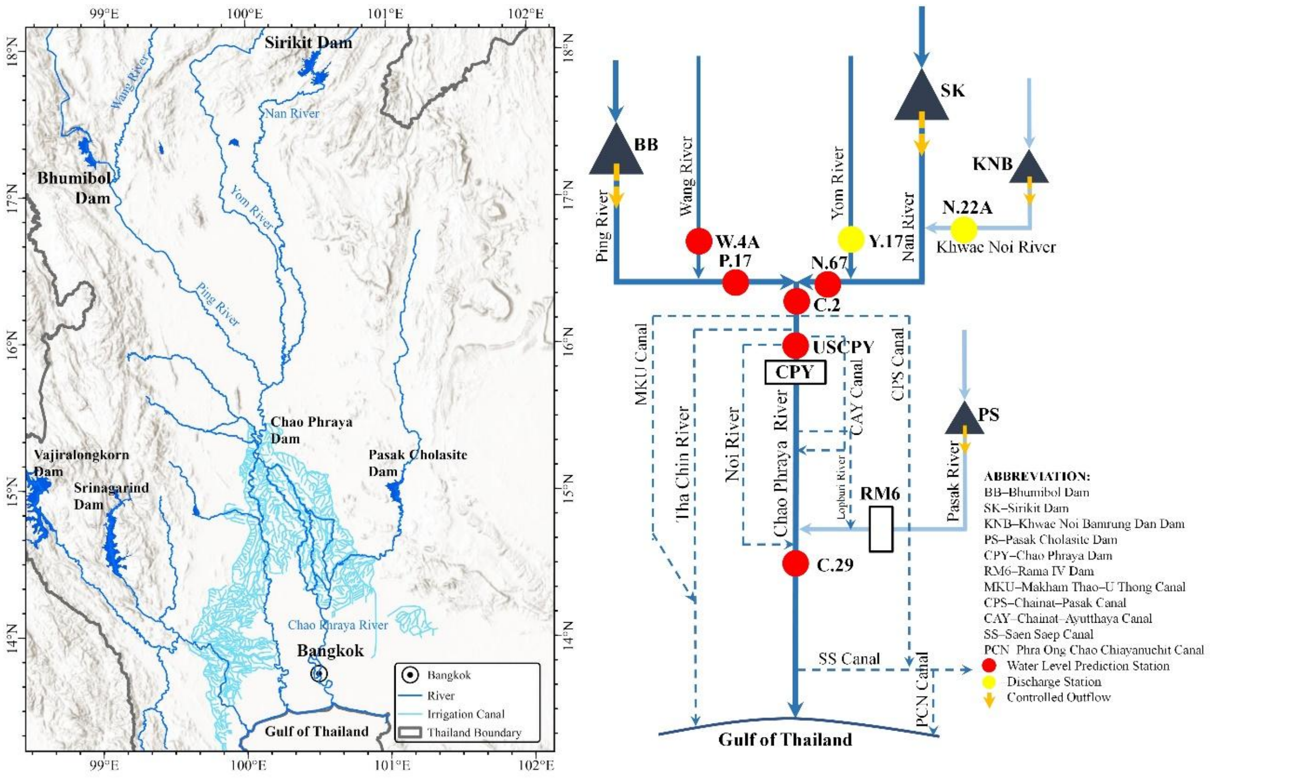

(a) Topographic map (b) River diagram and prediction stations

Fig. 1. The study area in the Choa Phraya River Basin.

Table 1. Data used for water level prediction modelling.

Data	Station Name	Data Type	Unit	Data Length
Sta. P.17	Ping River, Banphot Phisai District, Nakhon Sawan Province	Water level, Rainfall	m. msl., mm.	1/1/1999–31/10/2022
Sta. W.4A	Wang River, Sam Ngao District, Tak Province	Water level, Rainfall	m. msl., mm.	1/1/1993–30/6/2022
Sta. N.67	Nan River, Chum Saeng District, Nakhon Sawan Province	Water level, Rainfall	m. msl., mm.	1/1/2000–31/3/2023
Sta. C.2	Chao Phraya River, Mueang District, Nakhon Sawan Province	Water level, Rainfall	m. msl., mm.	1/1/2000–31/3/2023
USCPY	Upstream Chao Phraya Dam, Sapphaya District, Chai Nat Province	Water level, Rainfall	m. msl., mm.	1/1/2000–9/4/2021
Sta. C.29	Chao Phraya River, Bang Sai District, Phra Nakhon Si Ayutthaya Province	Water level, Rainfall	m. msl., mm.	1/6/2012–25/2/2022
RBB	Controlled Outflow from Bhumibol Dam	Controlled outflow	MCM	1/1/1999–31/3/2022
RSK	Controlled Outflow from Sirikit Dam	Controlled outflow	MCM	1/1/2009–31/3/2023
RKNB	Controlled Outflow from Khwae Noi Bumrung Dan Dam	Controlled outflow	MCM	1/1/2009–31/3/2023
RPS	Controlled Outflow from Pasak Cholasite Dam	Controlled outflow	MCM	1/6/2012–14/11/2020
QP.17	Discharge at Station P.17	Discharge	CMS	1/1/1999–31/3/2022
QW.4A	Discharge at Station W.4A	Discharge	CMS	1/1/1993–30/6/2022
QY.17	Discharge at Station Y.17	Discharge	CMS	1/1/2009–31/3/2023
QN.22A	Discharge at Station N.22A	Discharge	CMS	1/1/2009–31/3/2023
QN.67	Discharge at Station N.67	Discharge	CMS	1/1/2009–31/3/2023
QC.2	Discharge at Station C.2	Discharge	CMS	1/1/2000–31/3/2023
QUSCPY	Upstream discharge at Chao Phraya Dam	Discharge	CMS	1/1/2000–9/4/2021

Note: m. msl.–meter above mean sea level, MCM–Million Cubic Meter, CMS–Cubic Meter per Second

Table 2. Input features for one–day and one–week ahead water level prediction models.

Gauged Stations	Scenario Design	Model Types	Input Features												
			Water Level	Rainfall	Reservoir Outflow				Upstream Discharge						
					BB	SK	KNB	PS	P.17	W.4A	Y.17	N.22A	N.67	C.2	USCPY
t+1	–	–	t	t	t–1/t–2*	t–4	t–1	t	t	t–1	t	t–1	t	t	t–1
P.17	S1: XGBoost	Daily	✓	✓	✓	–	–	–	–	✓	–	–	–	–	–
	S2: RF	Daily	✓	✓	✓	–	–	–	–	✓	–	–	–	–	–
	S3: DNNs	Daily	✓	✓	✓	–	–	–	–	✓	–	–	–	–	–
	S4: XGBoost	Weekly	✓	✓	✓	–	–	–	–	✓	–	–	–	–	–
W.4A	S1: XGBoost	Daily	✓	✓	–	–	–	–	–	–	–	–	–	–	–
	S2: RF	Daily	✓	✓	–	–	–	–	–	–	–	–	–	–	–
	S3: DNNs	Daily	✓	✓	–	–	–	–	–	–	–	–	–	–	–
	S4: XGBoost	Weekly	✓	✓	–	–	–	–	–	–	–	–	–	–	–
N.67	S1: XGBoost	Daily	✓	✓	–	✓	✓	–	–	–	✓	✓	–	–	–
	S2: RF	Daily	✓	✓	–	✓	✓	–	–	–	✓	✓	–	–	–
	S3: DNNs	Daily	✓	✓	–	✓	✓	–	–	–	✓	✓	–	–	–
	S4: XGBoost	Weekly	✓	✓	–	✓	✓	–	–	–	✓	✓	–	–	–
C.2	S1: XGBoost	Daily	✓	✓	✓*	✓	✓	–	✓	–	✓	–	✓	–	–
	S2: RF	Daily	✓	✓	✓*	✓	✓	–	✓	–	✓	–	✓	–	–
	S3: DNNs	Daily	✓	✓	✓*	✓	✓	–	✓	–	✓	–	✓	–	–
	S4: XGBoost	Weekly	✓	✓	✓*	✓	✓	–	✓	–	✓	–	✓	–	–
USCPY	S1: XGBoost	Daily	✓	✓	–	–	–	–	–	–	–	–	–	✓	–
	S2: RF	Daily	✓	✓	–	–	–	–	–	–	–	–	–	✓	–
	S3: DNNs	Daily	✓	✓	–	–	–	–	–	–	–	–	–	✓	–
	S4: XGBoost	Weekly	✓	✓	–	–	–	–	–	–	–	–	–	✓	–
C.29	S1: XGBoost	Daily	✓	✓	–	–	–	✓	–	–	–	–	–	–	✓
	S2: RF	Daily	✓	✓	–	–	–	✓	–	–	–	–	–	–	✓
	S3: DNNs	Daily	✓	✓	–	–	–	✓	–	–	–	–	–	–	✓
	S4: XGBoost	Weekly	✓	✓	–	–	–	✓	–	–	–	–	–	–	✓

Note: Acronyms–Bhumibol Dam–BB | Sirikit Dam–SK | Khwae Noi Bamrung Dan Dam–KNB | Pasak Chonlasite Dam–PS | Upstream Chao Phraya Dam–USCPY | Scenarios–S1, S2, S3 Daily Prediction Models, S4 Weekly Prediction Model, t = Daily or Weekly Data

Table 3. Correlation coefficient between target water level at all gauged stations and selected input features.

Water Level at Gauged Stations	Correlation Coefficient												
	Water Level	Rainfall	Reservoir Outflow				Upstream Discharge						
			BB	SK	KNB	PS	P.17	W.4A	Y.17	N.22A	N.67	C.2	USCPY
t+1	t	t	t–1/t–2*	t–4	t–1	t	t	t–1	t	t–1	t	t	t–1
P.17	0.977	0.122	0.241	–	–	–	–	0.593	–	–	–	–	–
W.4A	0.983	0.183	–	–	–	–	–	–	–	–	–	–	–
N.67	0.997	0.223	–	0.045	0.422	–	–	–	0.801	0.266	–	–	–
C.2	0.998	0.202	0.043*	0.022	0.444	–	0.749	–	0.820	–	0.937	–	–
USCPY	0.986	0.121	–	–	–	–	–	–	–	–	–	0.563	–
C.29	0.856	0.230	–	–	–	0.598	–	–	–	–	–	–	0.854

Note: Acronyms–Bhumibol Dam–BB | Sirikit Dam–SK | Khwae Noi Bamrung Dan Dam–KNB | Pasak Chonlasite Dam–PS | Upstream Chao Phraya Dam–USCPY | t = Daily

2.2. ML Algorithms Selected

2.2.1. Extreme Gradient Boosting (XGBoost)

Extreme Gradient Boosting (XGBoost), a powerful ensemble machine learning algorithm based on sequential decision trees, was introduced by Tianqi Chen in 2014 [45]. XGBoost is an optimized version of gradient boosting utilizing several techniques in efficient way such as regularization, tree pruning, etc. [46]. Each tree in the XGBoost is trained sequentially aiming to minimize the prediction residuals made by the previous trees to achieve the better performance as graphically illustrated in Fig. 2(a). Due to its efficiency, scalability, and flexibility, XGBoost has been widely demonstrated and proven their performances for hydrological prediction applications [47, 48] such as reservoir inflow [49], river water level [10, 23, 33], flood event [50], groundwater level [34], etc.

In general, the supervised XGBoost learning primarily involves minimizing objective function which consists of two terms; (1) loss function and (2) regularization term as expressed in Eq. (1). This loss function measures the discrepancy between the predicted and observed values in the model training process. Selecting the loss function of XGBoost depends on the specific problems. For robust regression tasks, the common loss functions are Mean Squared Error (MSE) as given in Eq. (2), Mean Absolute Error (MAE), and Huber loss. The regularization term in Eq. (3) is used to prevent model overfitting and complexity for the improvement of prediction performance.

$$Obj(\theta) = L(\theta) + \Omega(\theta) \tag{1}$$

$$L(\theta) = \frac{1}{2}\sum_{i=1}^{n} (y_i - p_i)^2 \tag{2}$$

$$\Omega(\theta) = \gamma T + \frac{1}{2}\lambda \sum_{i=1}^{T} O_{value}^2 \tag{3}$$

where, $Obj(\theta)$, $(L(\theta))$, and $(\Omega(\theta))$ are objective function, loss function, and regularization term, respectively. θ represents the optimal parameter values that minimize the objective function resulting in the best fit of training process between the trained data (y_i) and the predicted output (p_i). γ is a controlled hyperparameter of the regularization term in tree–based learning models. This influences the decision to make a further partition on a leaf node of a tree–based model. The number of leaf nodes in the tree is denoted by T, which is a key factor controlling the model complexity. A larger number of leaf nodes can significantly enhance the overfitting risk. λ is a hyperparameter used to scale the regularization term. A larger λ indicates the increased penalty to model encouraging the reduction of model complexity. O_{value} is a measure of the diversity or dissimilarity of the data points within the leaf node. The tree structures are iteratively built for T iterations until the desired number of models is accomplished. In each iteration, the output value (O_{value}) for all leaf nodes is computed using Eq. (4).

$$O_{value} = \frac{\sum_{i=1}^{n} (y_i - p_i)}{n + \lambda} \tag{4}$$

The learning rate (ε) specifies magnitude of model adjustment to handle the prediction error made by previous iterations. It significantly governs the convergence speed and precision of the prediction model. A larger values of learning rate can speed up the training process leading to faster convergence and increased risk of overfitting. In contrast, the smaller values of learning rate can reduce risk of overfitting leading to the improved data generalization. However, it may require larger number of trees to achieve the same level of predication accuracy and the convergence speed is substantially lower. In the last step, XGBoost updates the prediction (p_i^t) by combining the initial prediction (p_i^0) value with a weighted sum of gradient of the loss function and the regularization term determined by the learning rate as expressed in Eq. (5).

$$p_i^t = p_i^0 + \varepsilon\left[\sum_{i=1}^{n} L\,(y_i, p_i^0 + O_{value}) + \frac{1}{2}\lambda O_{value}^2\right] \tag{5}$$

2.2.2. Random Forest (RF)

Random Forest (RF) is multiple decision tree–based ensemble machine learning algorithm widely applied for both regression and classification problems. It was introduced by Breiman in 2001 [51]. RF creates multiple decision trees by training each on a random sample of training data and average their predictions to make the final prediction as depicted in Fig. 2(b). As the number of trees in RF increases, model performance generally stabilizes which helps to reduce the risk of overfitting [52]. RF can also excel in capturing the non–linearity system within the data. Furthermore, small number of the model parameters in RF makes the implementation easy [53]. The room for growth of RF algorithm has been applied for water science and hydrological applications such as water level [33, 45, 54], sea level [56], flood discharge simulation [53], reservoir inflow [55, 56].

2.2.3. Deep Neural Networks (DNNs)

Deep Neural Networks (DNNs) is a type of Artificial Neuron Networks (ANNs) broadly applied for regression, classification, and patter recognition problems. DNNs has been employed for both short–term and long–term predictions of hydrological data such as river water level [57], river tide level [58], reservoir water level [59]; rainfall [60], runoff [61], and river water temperature [62], etc. Generally, DNNs comprises multiple hidden layers of fully interconnected neurons that perform a series of complex transformations on input data implemented by activation functions to generate the predicted output as shown in Fig. 2(c). The deeper DNNs architectures with multiple layers have demonstrated superior precise prediction in capturing complex relationships between input and output variables. The crucial parameters identifying the DNNs architectures and training are number of layers, number of neurons in each layer, connection weights between neurons, the choice of activation function employed, epochs, batch size, and validation split. The background of DNNs is basically rooted in the foundation of ANNs. The predicted output is determined as a function of input data through the application of activation functions or y = f(x) where x is input data and y is predicted output. The relationship between inputs and outputs within the hidden layers of DNNs is expressed in Eq. (6).

$$y = g\left(\sum_i w_i x_i + b\right) \tag{6}$$

where the output of neuron i^{th} from the previous layer is denoted as x_i, the weight between the present and neuron i^{th} is represented as w_i. Each neuron in hidden layer calculates a weighted sum of inputs from the previous layer with the added bias value (b) that is initialized with random values. Activation function (g) is then employed resulting in the output for the specific neuron. The typical activation functions of DNNs are sigmoid, tanh, and ReLu (Rectifier Linear Unit) to introduce non–linearity [58]. Sigmoid function maps the input values to output range between 0 and 1 producing a smooth S–shaped curve as expressed in Eq. (7). The tanh function in Eq. (8) outputs the values in a range of –1 to 1. The ReLu function replaces the negative value with 0 as given in Eq. (9).

$$sigm(x) = \frac{1}{1+e^{-x}} \tag{7}$$

$$tanh(x) = 2\sigma(2x)-1 \tag{8}$$

$$f(x) = max(0, x) \tag{9}$$

2.3. Model Training and Testing

The model training and testing of the daily and weekly prediction models were conducted for one–day ahead and one–week ahead water level predictions at six gauged stations. As previously mentioned, selecting the combination of input features was carried out and structured in the water level prediction models based on the physical river–reservoir system using past water level, rainfall, controlled outflow by upper reservoirs, and upstream discharges with different travel times. Python–a programming language with three ML algorithms; XGBoost, RF, and DNNs, was used for the development of the water level prediction models. Hyperparameter tuning for different prediction scenarios was then implemented.

Key hyperparameters of XGBoost algorithm include learning rate, number of trees (or boosting rounds), maximum depth of each tree, and regularization parameters to prevent overfitting. However, two main hyperparameters that had a significant impact on the predictions were identified in this study; (1) learning rate, which was tested from 0.001 to 0.3, and (2) number of estimators (n–estimators), which ranged from 100 to 500. Grid search cross–validation using the "GridsearchCV" library was also executed for hyperparameter tuning.

RF was selected in the context of predicting water levels in a river in this study. Key hyperparameters of RF including n–estimators, maximum tree depth, minimum samples leaf, and minimum sample split, were accordingly tuned. Number of estimators were ranged from 50 to 200, maximum tree depth from 10 to 30, minimum samples per leaf from 1 to 4, and minimum samples per split from 2 to 10.

DNNs, Deep Neural Networks was also selected to predict the river water level as it can learn complex relationship of large datasets. In this study, ReLU was used as it is well–suited for regression problems. The network undergoes a training process involving forward propagation, where data is passed through the network to produce predictions, followed by the calculation of a loss function. The backpropagation process then adjusts weights and biases using gradient descent to minimize loss and improve the network's performance. To minimize the loss function during the model training, adam optimizer which is an adaptive learning rate algorithm, was accordingly used.

After that the best training model in prediction by each algorithm using 80% of dataset was obtained and testing model was then conducted using the best model parameters and remaining 20% of dataset.

2.4. Evaluation of Model's Predictive Performance

Evaluating the model's performance includes a comparison of the predicted values with the actual water level values from both the training and testing datasets. The statistical metrics used in this study are as follows; R–squared (R^2), Mean Absolute Error (MAE), Mean Squared Error (MSE), and Root Mean Squared Error (RMSE). To fulfill a complete picture of the calculation process of prediction errors and model verification, both MSE and RMSE which are critical metrics for prediction models, were accordingly presented in this study. The R^2, a dimensionless metric, measures the proportion of the variance in the target variable that is explained by the model. A higher R^2 value closer to 1 indicates better predictive power. The units for MAE and RMSE are meters (m), while the unit for MSE is meters squared (m^2). These metrics quantify the absolute and squared differences between the predicted and actual values. A lower value of MAE, MSE, and RMSE indicates better model performance. In this study, these evaluation metrics were calculated using Python library "sklearn" metrics. In the last step, the model's capability to predict daily low and high water levels was assessed to leverage the application of ML for flood and drought monitoring during the critical periods. The lowest and highest values of water levels in each month of the tested results were compared to the observed water levels. Finally, average percentage error in prediction was computed. The overall workflow of this study is depicted in Fig. 3.

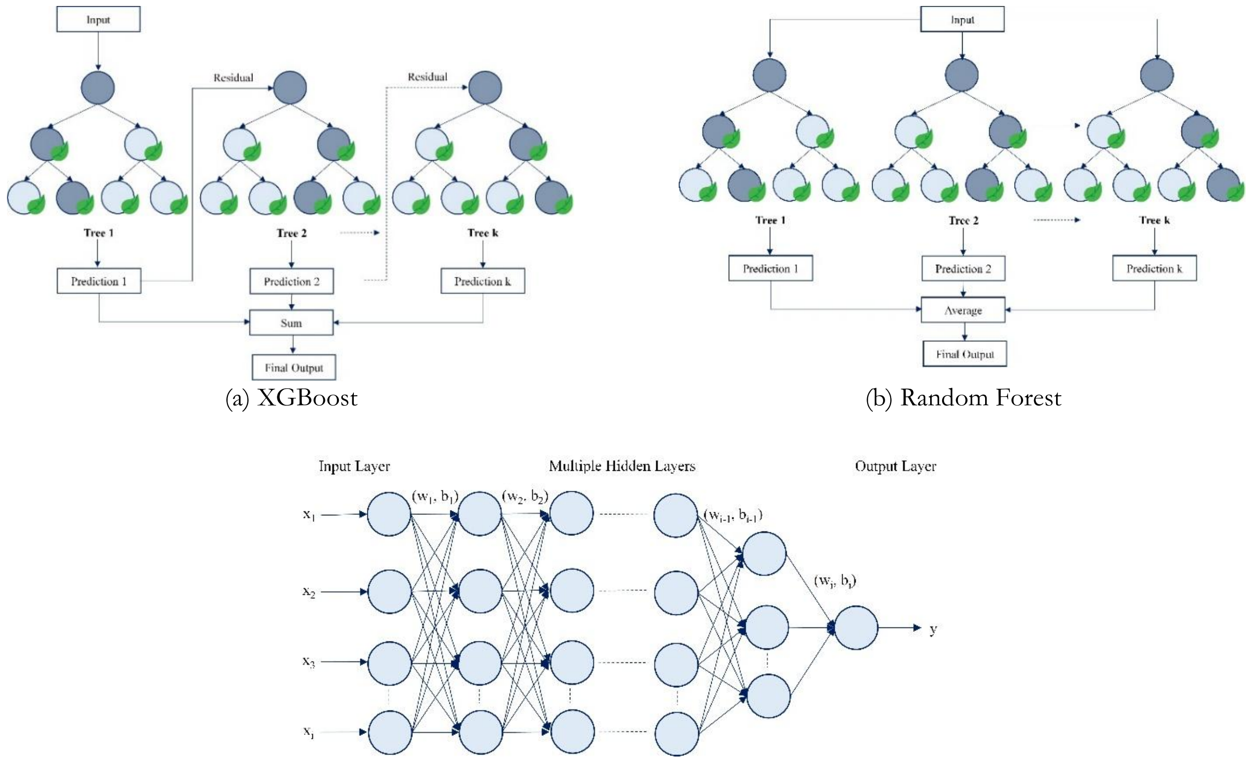

(a) XGBoost (b) Random Forest

(c) Deep Neural Networks

Fig. 2. Simplified structures of ML prediction models.

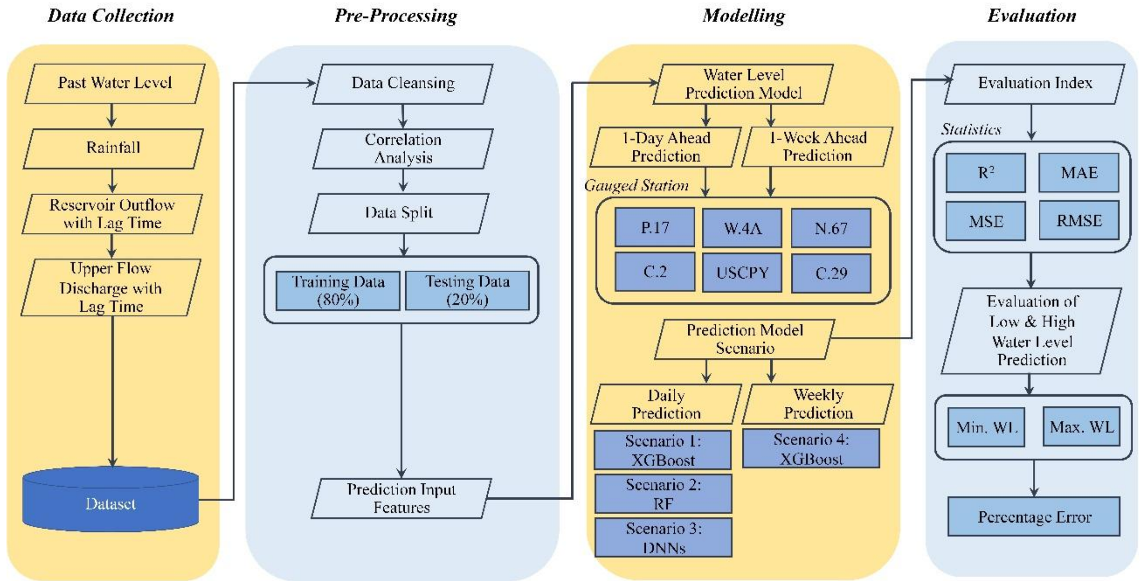

Fig. 3. Workflow diagram of this study.

3. Results and Discussion

3.1. Hyperparameter Tuning for the Optimal Different Prediction Scenarios

Hyperparameter tuning for the optimal different prediction scenarios was implemented in a way of minimizing MSE across 5–fold cross–validation to prevent overfitting during the training process as summarized in Table 4. Scenario 1, XGBoost–based daily prediction revealed that the learning rate of 0.1 was optimal for most gauged stations including Stations W.4A, N.67, C.2, USCPY, and C.29. However, Station P.17 demonstrated the optimal learning rate of 0.01. For the Scenario 4, XGBoost–based weekly prediction exhibited the optimal learning rates of 0.01 for four gauged stations including Stations P.17, W.4A, USCPY, and C.29. Whereas, the bigger values of learning rates of 0.1 and 0.2 were optimal for Stations N.67 and C.2, respectively. This key finding highlighted that optimal learning rates indicating the balance between the training speed and risk of overfitting of XGBoost algorithm for water level prediction predominantly lied in the range of 0.01 to 0.1. The number of estimators (n–estimators) determining the number of decision trees to be sequentially built is also one of the significant hyperpameter of XGBoost. The analysis revealed that the n–estimators varying from 100 to 500 were optimal for all gauged stations to effectively control the model complexity. However, the lower n–estimators of 100 were well–performed in daily prediction model which typically incorporated larger datasets. Conversely, the bigger n–estimators of 500 were suited for weekly prediction model characterized by smaller datasets. This finding suggests that XGBoost–based prediction model exploiting smaller datasets like weekly or monthly model may require the higher number of n–estimators to achieve the better predictive performance. However, higher values of n–estimators substantially increased the computational resources and training time.

Table 4. Hyperparameter tuning for the optimal different prediction scenarios.

Gauged Stations	Scenario 1: XGBoost_daily model	Scenario 2: RF_daily model	Scenario 3: DNNs_daily model	Scenario 4: XGBoost_weekly model
P.17	learning rate: 0.01 n–estimators: 500	n–estimators: 100 max. depth: 10 min. samples leaf: 4 min. samples split: 10	learning rate: 0.001 epochs: 50 batch size: 32 validation split: 0.2 activation: relu	learning rate: 0.01 n–estimators: 400
W.4A	learning rate: 0.10 n–estimators: 100	n–estimators: 100 max. depth: 10 min. samples leaf: 4 min. samples split: 10	learning rate: 0.001 epochs: 50 batch size: 32 validation split: 0.2 activation: relu	learning rate: 0.01 n–estimators: 500
N.67	learning rate: 0.10 n–estimators: 100	n–estimators: 100 max. depth: 10 min. samples leaf: 4 min. samples split: 10	learning rate: 0.001 epochs: 50 batch size: 32 validation split: 0.2 activation: relu	learning rate: 0.10 n–estimators: 100
C.2	learning rate: 0.10 n–estimators: 200	n–estimators: 150 max. depth: 10 min. samples leaf: 2 min. samples split: 2	learning rate: 0.001 epochs: 50 batch size: 32 validation split: 0.2 activation: relu	learning rate: 0.20 n–estimators: 300
USCPY	learning rate: 0.10 n–estimators: 100	n–estimators: 150 max. depth: 10 min. samples leaf: 4 min. samples split: 2	learning rate: 0.001 epochs: 50 batch size: 32 validation split: 0.2 activation: relu	learning rate: 0.01 n–estimators: 500
C.29	learning rate: 0.10 n–estimators: 100	n–estimators: 150 max. depth: 10 min. samples leaf: 2 min. samples split: 10	learning rate: 0.001 epochs: 50 batch size: 32 validation split: 0.2 activation: relu	learning rate: 0.01 n–estimators: 500

Scenario 2, RF–based daily prediction demonstrated that designated n–estimators of 100 and 150 yielded the good predictive performance for all gauged stations. The maximum tree depth of 10 which is the lowest designed values controlling the complexity of the individual decision trees within the forest, gave the best predictive results for all gauged stations. Moreover, the maximum designated values for minimum samples per leaf and minimum samples per split which were 4 and 10, respectively, were found to be optimal for all gauged stations in controlling the tree size and model complexity. Among key hyperparameters of RF algorithm, number of estimators had a significant impact on the training performance compared to maximum tree depth, minimum samples per leaf, and minimum samples per split. Compared to XGBoost, the training time of RF–based daily prediction was longer.

Scenario 3, DNNs–based daily prediction for Station P.17 exhibited that the optimal values of key hyperparameters of DNNs including learning rate, number of epochs, batch size, and validation split are 0.001, 50, 32, and 0.2, respectively. The learning rate is a crucial hyperparameter initially set to control step size taken for efficient training. The number of epochs determines the number of times during training process that entire training datasets are completely passed through the networks. The batch size directly influences the number of training examples in each parameter's update. In this study, these hyperparameters were subsequently applied to other flow gauged stations for comparative analysis in term of their predictive performances. In addition, DNNs–based daily prediction exhibited the longest training time compared to XGBoost and RF due to complex architecture with multiple hidden layers of interconnected nodes of DNNs. This resulted in increased training time since a larger number of parameters needed to be learned during training process.

3.2. Predicted One–Day and One–Week Ahead Water Levels of All Gauged Stations

The predictive results of the one–day and one–week ahead water levels at P.17, W.4A, N.67, C.2, USCPY, and C.29 gauged stations are shown in Fig. 4 and the statistical performances are presented in Table 5. To implicitly visualize and compare the statistically predictive performance metrics between daily models and weekly model, radar chart comparing R^2, MAE, MSE, and RMSE values for four prediction model scenarios is presented as graphically shown in Fig. 5. It is exhibited that three daily model scenarios (S1, S3, and S3) for one–day ahead water level prediction robustly and consistently outperformed the weekly prediction model (S4) across different key gauged stations. With exception of Station C.29, these daily prediction models achieved strong R^2 values ranging from 0.937 to 0.999 for model training and from 0.958 to 0.994 for model testing, making it effective for water level short–term forecasting. The weekly prediction model, optimized for weekly time intervals across all gauged stations, showed potentially lower R^2 values of 0.814 to 0.999 for model training and 0.600 to 0.693 for model testing. Higher MAE, MSE, RMSE values were observed ranging from 0.002 to 0.580 meter for model training and 0.015 to 0.670 meter for model testing due to the challenges of forecasting over a period. Since Station C.29 is located downstream of CPY dam where localized flow and sea tidal backwater encroaching from the Gulf of Thailand [63] are significant factors, this leads to the high fluctuation in water level. Consequently, it showed lower R^2 values of 0.600–0.786 and higher MAE, MSE, RMSE values ranging from 0.011 to 0.122 meter for the model testing in all prediction scenarios compared to other gauged stations. Moreover, since the inputs of weekly model were averaged from daily water level data, this influences model's predictability to capture disturbed variability and seasonality. The choice between daily and weekly prediction models depends on the specific forecasting needs of the decision makers. Generally, the daily model excels in real–time monitoring, while the weekly model is used for strategic planning.

This study also explored various modelling ML algorithms including XGBoost, RF, and DNNs, to predict one–day ahead and one–week ahead water levels at key gauged stations when applied for testing dataset. The Scenario 1 using XGBoost algorithm, showed high accuracy at Stations N.67 and C.2 when trained with rainfall data, though it faces challenges at Station C.29 due to non–seasonal variation of water level data. With rainfall data, XGBoost highly improved the precision at some stations particularly at Station P.17, though the overall performance varied with certain stations showing no significant changes. The Scenario 2 using RF algorithm exhibited similar stability with testing errors closely aligning with training errors, indicating good model robustness. It slightly outperformed in comparison to XGBoost, particularly at Stations P.17, C.2 and USPCY, but required longer training times and produced mixed results across different stations. The Scenario 3 using DNNs algorithm generally performed well with high R^2, especially at Stations P.17 and W.4A. However, they still face challenges in some stations with non–seasonal variation in water levels like Station C.29.

This study underscores the importance of selecting the most appropriate modeling approach based on the specific physical characteristics of the gauged stations and the prediction objectives. Among ML algorithms used in this study for water level prediction at six gauged stations, tree–based XGBoost and RF models, with rainfall input maintains consistent performance, reflecting their ability to generalize well to unanticipated data for all the gauged stations. In other words, XGBoost and RF algorithms provide the closer predictive performances for both daily and weekly water level predictions. While DNNs, a deep fully connected NN model, requires optimization to enhance their generalization capabilities as the bigger MAE, MSE, and RMSE values were found at some gauged stations particularly at Stations W.4A and USCPY.

3.3. Evaluation of Low Water Level and High Water Level Prediction

As previously mentioned, the ML algorithms applied to the daily water level prediction models for three scenarios can capture the entire testing dataset with high precision than weekly prediction model. Accordingly, the average percentage error of the lowest water level (Min. WL) and highest water level (Max. WL) for daily prediction was assessed. This error calculation was made for all gauged stations by comparing the lowest and highest daily observed water level values for each month within the testing dataset periods against the daily predicted values in the corresponding time periods. The comparative results between observed and predicted values of both low and high water levels are presented in Fig. 6 and Table 6.

It is revealed that these three ML prediction models consistently exhibited a small positive average percentage error of overestimating low water levels. For all gauged stations except Scenario 3 of USCPY showing negative percentage errors, these errors lied closely to the observed low water level from +0.0088% to +0.9380%, +0.0089% to +0.7288%, and +0.0289% to +0.7652%, for Scenario 1, Scenario 2, and Scenario 3, respectively. However, high average percentage error was obviously found at Station C.29 by +31.8743%, +11.6832%, and +12.3576%, respectively for these three scenarios as high fluctuation of unanticipated localized flow is a key influential factor. Among ML algorithms employed, RF demonstrated the best predictive performance for low water level prediction exhibiting the smallest percentage error found at most gauged stations.

For the high water level prediction, these three ML models showed both positive and negative values of average percentage errors with small percentage error lying from –0.7995% to +0.4583%, –0.1046% to +1.1587%, and –2.2696% to +0.6018% for Scenario 1, Scenario 2, and Scenario 3, respectively. This indicated underestimating particularly at Stations P.17 and USCPY and overestimating at Stations N.67 and C.2 for all scenarios. All in all, these three ML algorithms; XGBoost, RF, and DNNs, demonstrated high predictive performance level for high water level prediction.

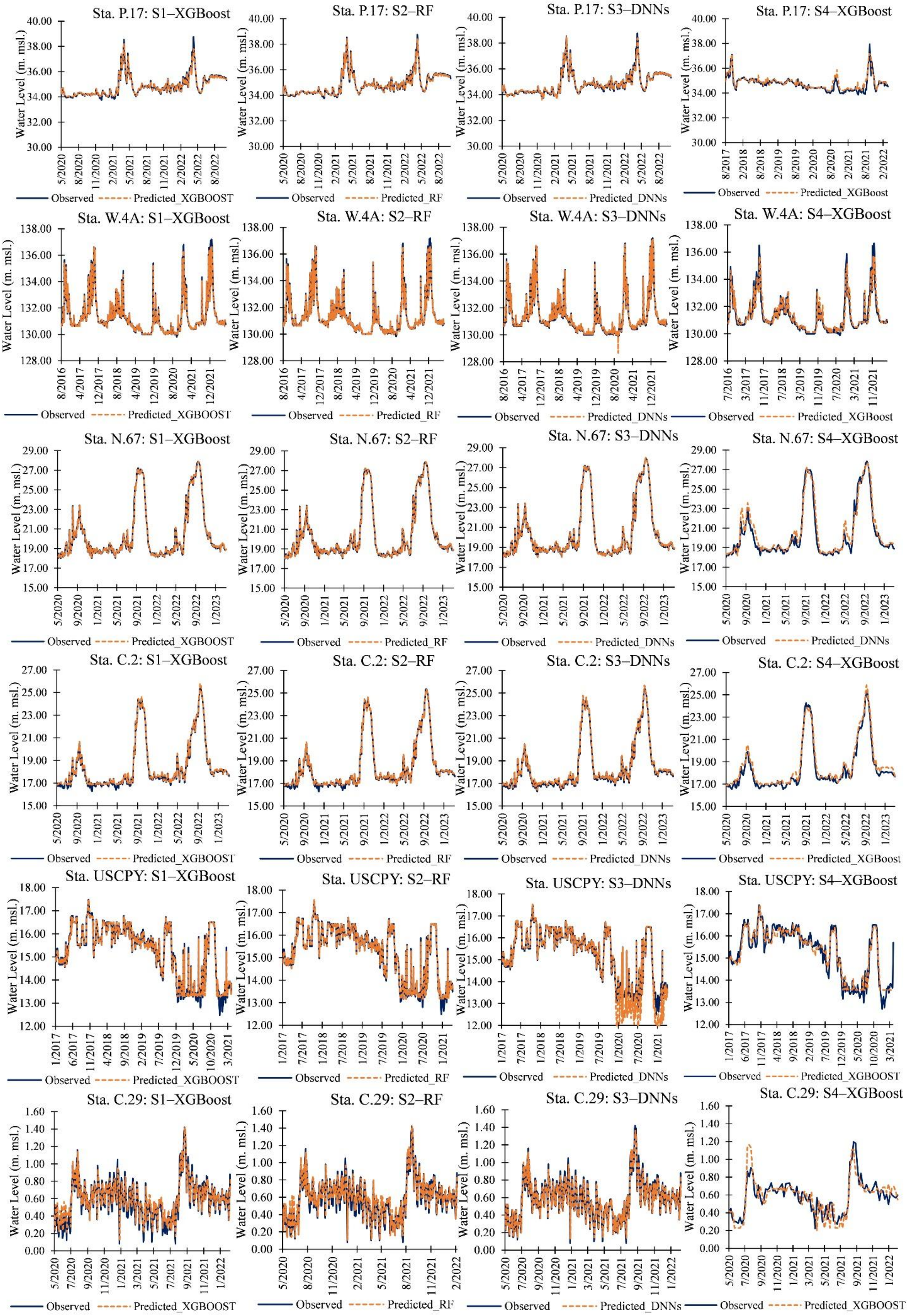

Fig. 4. Predicted one–day ahead water levels for daily prediction scenarios (S1, S2, S3) and one–week ahead water levels for weekly prediction scenario (S4) across all gauged stations.

Table 5. Statistical performances of predicted water levels at key gauged stations–training and testing data set.

Water Level Prediction Models			Gauged Stations					
Scenario Design	Model Building	Statistical Metrics	P.17	W.4A	N.67	C.2	USCPY	C.29
S1: Daily model using XGBoost algorithm with rainfall	Training	R^2	0.957	0.971	0.995	0.999	0.978	0.969
		MAE	0.088	0.119	0.119	0.055	0.072	0.072
		MSE	0.018	0.056	0.028	0.005	0.014	0.009
		RMSE	0.135	0.236	0.168	0.074	0.118	0.093
	Testing	R^2	0.961	0.958	0.994	0.994	0.961	0.760
		MAE	0.097	0.135	0.132	0.123	0.106	0.082
		MSE	0.024	0.078	0.042	0.027	0.052	0.012
		RMSE	0.165	0.280	0.206	0.163	0.228	0.109
S2: Daily model using RF algorithm with rainfall	Training	R^2	0.968	0.978	0.997	0.999	0.984	0.980
		MAE	0.075	0.104	0.092	0.043	0.060	0.058
		MSE	0.013	0.041	0.018	0.004	0.010	0.006
		RMSE	0.115	0.203	0.134	0.062	0.101	0.075
	Testing	R^2	0.966	0.958	0.994	0.995	0.966	0.743
		MAE	0.087	0.137	0.132	0.118	0.096	0.087
		MSE	0.023	0.078	0.043	0.026	0.047	0.013
		RMSE	0.153	0.279	0.206	0.162	0.216	0.113
S3: Daily model using DNNs algorithm with rainfall	Training	R^2	0.937	0.967	0.995	0.997	0.973	0.967
		MAE	0.109	0.120	0.119	0.079	0.081	0.074
		MSE	0.026	0.062	0.031	0.011	0.017	0.009
		RMSE	0.162	0.250	0.175	0.106	0.132	0.096
	Testing	R^2	0.994	0.960	0.994	0.995	0.851	0.786
		MAE	0.133	0.128	0.132	0.120	0.236	0.077
		MSE	0.042	0.076	0.043	0.023	0.203	0.011
		RMSE	0.205	0.277	0.206	0.153	0.451	0.103
S4: Weekly model using XGBoost algorithm with rainfall	Training	R^2	0.870	0.814	0.981	0.999	0.883	0.959
		MAE	0.155	0.354	0.238	0.033	0.204	0.083
		MSE	0.050	0.336	0.115	0.002	0.071	0.011
		RMSE	0.223	0.580	0.339	0.044	0.267	0.104
	Testing	R^2	0.704	0.770	0.940	0.963	0.908	0.600
		MAE	0.227	0.380	0.485	0.338	0.258	0.093
		MSE	0.116	0.403	0.447	0.174	0.121	0.015
		RMSE	0.341	0.635	0.670	0.417	0.348	0.122

Note: R^2 is dimensionless | Units for MAE and RMSE are meters (m) | Unit for MSE is meters squared (m^2)

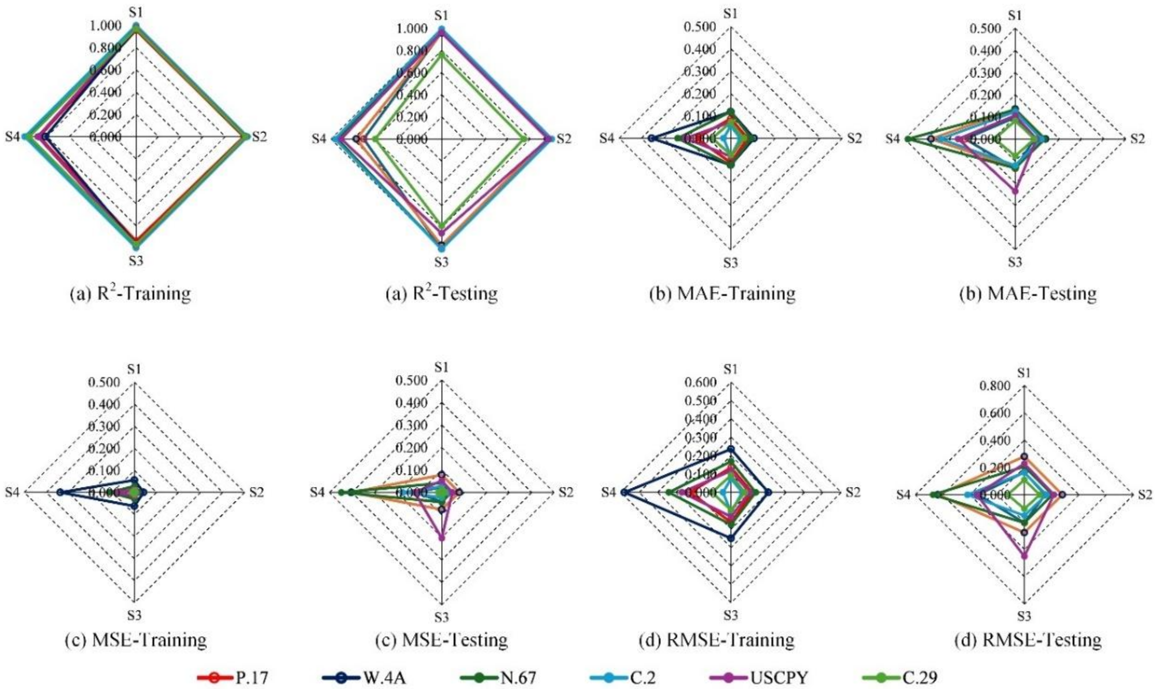

Fig. 5. Radar chart comparing the predictive performance metrics between daily models (S1, S2, and S3) and weekly model (S4).

Table 6. Percentage error of low water level and high water level prediction.

Gauged Station	Testing Period	Avg. %Error: S1–XGBoost		Avg. %Error: S2–RF		Avg. %Error: S3–DNNs	
		Min. WL	Max. WL	Min. WL	Max. WL	Min. WL	Max. WL
P.17	1/5/2020–31/10/2022	+0.1382%	–0.1611%	+0.0761%	–0.0405%	+0.0709%	–0.0296%
W.4A	5/8/2016–30/6/2022	+0.0088%	–0.0207%	+0.0089%	–0.0035%	+0.0289%	+0.0397%
N.67	1/5/2020–31/3/2023	+0.2660%	+0.0430%	+0.2140%	+0.0779%	+0.3062%	+0.1347%
C.2	1/5/2020–31/3/2023	+0.9380%	+0.4583%	+0.7288%	+0.3055%	+0.7652%	+0.6018%
USCPY	7/1/2017–9/4/2021	+0.5633%	–0.1636%	+0.3271%	–0.1046%	–2.1512%	–0.0804%
C.29	20/5/2020–25/2/2022	+31.8743%	–0.7995%	+11.6832%	+1.1587%	+12.3576%	–2.2696%

DOI:10.4186/ej.2025.29.8.147

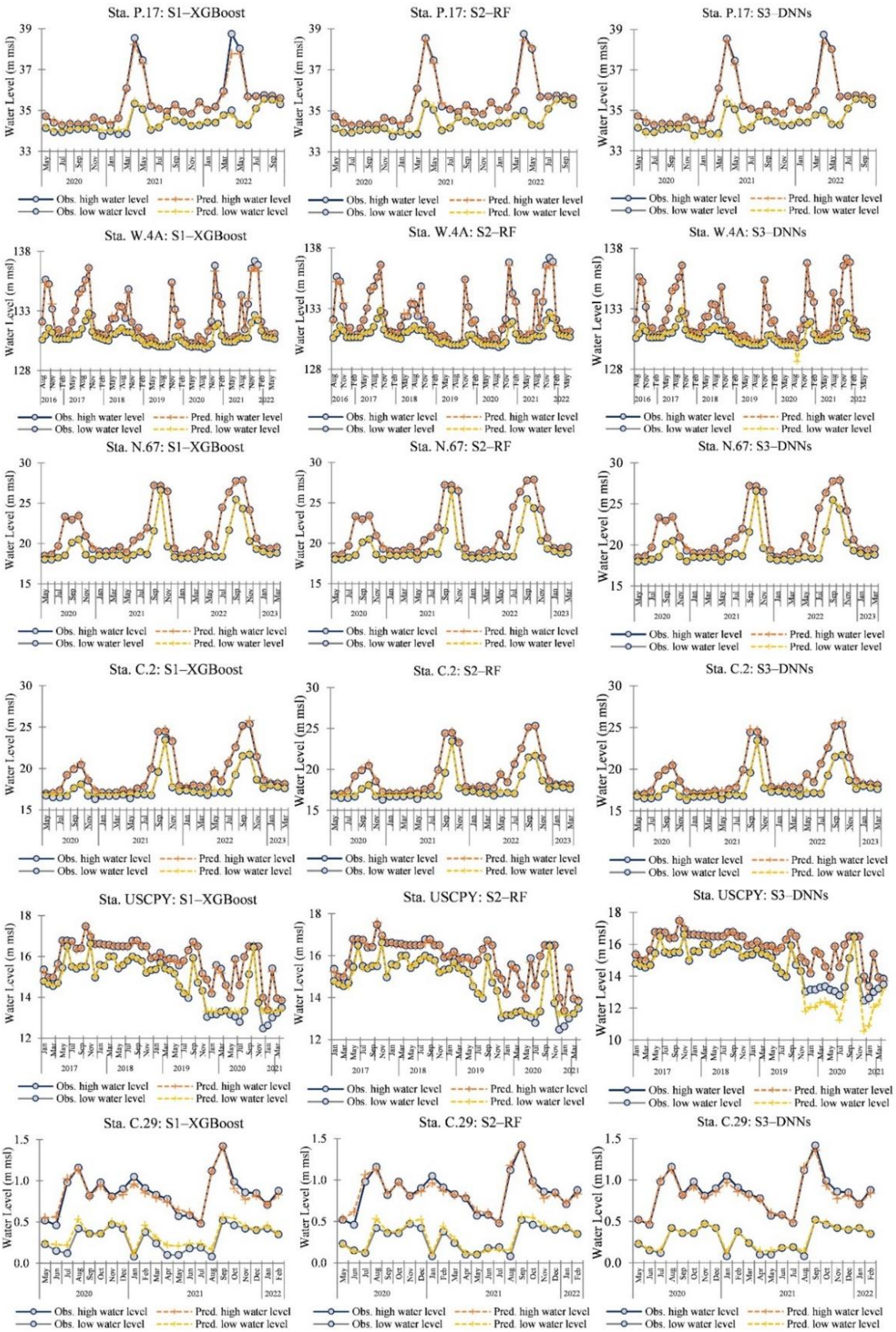

Fig. 6. Comparison of low water level and high water level prediction.

3.4. Performance Evaluation and Model Limitations

The daily prediction from the ML–based water level models offer valuable and real–time insights for decision–makers. The predictive results of changing water levels aid informed decisions for proper water allocation in dry periods, and anticipating daily fluctuations in water levels during storm periods. This capability enables proactive measures for real–time flood and drought monitoring and disaster preparedness which will enhance resilience to extreme weather events. The weekly prediction from the ML–based water level models prove instrumental in anticipating periodic surges in water level and provides more profound insights into long–term average behavior of water levels, thereby aiding more sophisticated water resource management strategies.

Daily prediction models employing XGBoost, RF, and DNNs showed exceptional predictive capabilities, particularly in specific stations (P.17, N.67, C.2) where high R^2 values and lower error metrics were observed. These models leveraged sophisticated techniques to capture complex data relationships and achieve precise water level predictions particularly when input variables were tailored to station–specific characteristics. While weekly prediction models presented unique challenges of capturing longer–term trends and variation, they demonstrated moderate to good fit for all gauged stations with varying degrees of predictive accuracy. Furthermore, integrating rainfall data into daily and weekly prediction models underscored the importance of feature selection and showed the increased accuracy. Moreover, ML–based water level prediction models performed effectively for all gauged stations with significant fluctuation and dynamic water level patterns. In contrast, gauged stations with uniform water level data did not perform well with ML–based prediction models, as lower predictive accuracy was often displayed. Consequently, there is room for improvement by using time–series–specific ML models, such as Recurrent Neural Networks (RNN), Long Short–Term Memory (LSTM) networks, or Gated Recurrent Units (GRU), to better capture temporal dependencies in the data. An alternative hybrid modeling approach could also be explored to achieve more accurate forecasts. Importantly, separating flood and non–flood events [64] to conduct water level prediction scenarios could be an optional strategy to further enhance model capabilities. For applicable use particularly during extreme weather events, model training strategies by fine–tuning on extreme event data are recommended after initial training on the full data are accomplished. In addition, selecting robust optimizers which are less sensitive to outliers are also suggested to enhance predictive capabilities. Furthermore, incorporating multi–step prediction [65] into both daily models such as t+1, t+2, …., t+7 and weekly models such as t+1, t+2, …., t+4 will greatly leverage their utility for hydrological forecasting and effective water management.

4. Conclusion

This research assessed capability of ML models including XGBoost, RF, and DNNs to predict water levels at key gauged stations along the Chao Phraya River and its major tributaries aiding in flood and drought monitoring and mitigation. The findings revealed that three scenarios of daily models for one–day ahead real–time prediction showed superior accuracy in terms of statistical metrics as it can capture the entire testing dataset well with high precision than the weekly model. Compared to daily models, weekly model for one–week ahead water level prediction particularly for short–term strategic planning task is underperformed for all gauged stations. Both three–based XGBoost and RF models with rainfall input apparently exhibits consistent performance than DNNs, a deep fully connected NN model, reflecting their ability to generalize well to unanticipated data for the entire dataset at all the gauged stations. In addition, RF demonstrates the best predictive performance for low water level prediction exhibiting the smallest percentage error of overestimating found at most gauged stations compared to XGBoost and DNNs. However, these three ML algorithms; XGBoost, RF, and DNNs, demonstrate high predictive performance level for high water level prediction as it shows small percentage error of both overestimating and underestimating at some gauged stations. Moreover, it is apparent that ML prediction models show higher effectiveness for all gauged stations with water level behaviors significantly varied by seasonal effect, while gauged stations with stable levels benefitted less. This indicates that ML–based predictive performance is closely linked to the seasonal variability in water level data. Therefore, alternative prediction approaches may be necessary for stations exhibiting uniform water levels. Daily predictions by ML models offer valuable real–time insights for water resource management, particularly for signaling daily water levels during critical flood and drought periods. However, weekly prediction assists in strategic planning for addressing challenges in diverse hydrological environments and efficient water use across reservoirs.

Acknowledgement

The authors are grateful to the Royal Irrigation Department (RID) and Electricity Generating Authority of Thailand (EGAT) for providing research data.

References

[1] C. Deng, P. Sun, X. Yin, J. Zou, and W. Wang, "Assessment of monthly simulations based on a physics–informed machine learning framework: The effect of intermediate variables in its construction," *J. Environ. Manage.*, vol. 362, no. 121299, 2024, doi: 10.1016/j.jenvman.2024.121299.

[2] S. Swagatika, J. C. Paula, B. B. Sahoob, S. K. Guptac, and P. K. Singh, "Improving the forecasting accuracy of monthly runoff time series of the Brahmani River in India using a hybrid deep learning model," *J. Water Clim. Change*, vol. 15, no. 1, pp. 139-156, 2023, doi: 10.2166/wcc.2023.487.

[3] S. Alvisi, G. Mascellani, M. Franchini, and A. B´ardossy, "Water level forecasting through fuzzy logic and artificial neural network approaches," *HESS*, vol. 10, pp. 1–17, 2006, doi: 10.5194/hess-10-1-2006.

[4] L. Z. Mase, K. Amri, M. Farid, F. Rahmat, M. N. Fikri, J. Saputra, and S. Likitlersuang, "Effect of water level fluctuation on riverbank stability at the estuary area of Muaro Kualo Segment, Muara Bangkahulu River in Bengkulu, Indonesia," *Engineering Journal*, vol. 26, no. 3, pp. 1–16, Mar. 2022, doi: 10.4186/ej.2022.26.3.1.

[5] T. S. Nguyen, K. Ngamcharoen, and S. Likitlersuang, "Statistical characterisation of the geotechnical properties of Bangkok Subsoil," *Geotech. Geol. Eng.*, vol. 41, pp. 2043–2063, 2023, doi: 10.1007/s10706-023-02390-z.

[6] M. F. Qodri, L. Z. Mase, and S. Likitlersuang, "Non–linear site response analysis of Bangkok subsoils due to earthquakes triggered by three pagodas fault," *Engineering Journal*, vol. 25, no. 1, pp. 43–52, Jan. 2021, doi: 10.4186/ej.2021.25.1.43.

[7] A. Hipni, A. El–shafie, A. Najah, O. A. Karim, A. Hussain, and M. Mukhlisin, "Daily forecasting of dam water levels: Comparing a support vector machine (SVM) model with adaptive neuro fuzzy inference system (ANFIS)," *Water Resour. Manag.*, vol. 27, no. 10, pp. 3803–3823, 2013, doi: 10.1007/s11269–013–0382–4.

[8] R. Dai, W. Wang, R. Zhang, and L. Yu, "Multimodal deep learning water level forecasting model for multiscale drought alert in Feiyun River basin," *Expert Syst. Appl.*, vol. 244, no. 122951, 2024, doi: 10.1016/j.eswa.2023.122951.

[9] S. Dazzi, R. Vacondio, and P. Mignosa, "Flood stage forecasting using machine–learning methods: A case study on the Parma river (Italy)," *Water (Basel)*, vol. 13, no. 1, p. 1612, 2021, doi: 10.3390/w13121612.

[10] M. N. A. Zakaria, A. N. Ahmed, M. A. Malek, A. H. Birima, M. M. H. Khan, M. Sherif, and A. Elshafie, "Exploring machine learning algorithms for accurate water level forecasting in Muda river, Malaysia," *Heliyon*, vol. 9, p. e17689, 2023, doi: 10.1016/j.heliyon.2023.e17689.

[11] Z. Wang, N. Xu, X. Bao, J. Wu, and X. Cui, "Spatio-temporal deep learning model for accurate streamflow prediction with multi-source data fusion," *Environ. Model Softw.*, vol. 178, p. 106091, 2024, doi: 10.1016/j.envsoft.2024.106091.

[12] T. Zhoua, Z. Jiangb, X. Liuc, and K. Tan, "Research on the long–term and short–term forecasts of navigable river's water–level fluctuation based on the adaptive multilayer perceptron," *J. Hydrol.*, vol. 591, p. 125285, 2020, doi: 10.1016/j.jhydrol.2020.125285.

[13] F. Gurbuz, A. Mudireddy, R. Mantilla, and S. Xiao, "Using a physics–based hydrological model and storm transposition to investigate machine–learning algorithms for streamflow prediction," *J. Hydrol.*, vol. 628, p. 130504, 2024, doi: 10.1016/j.jhydrol.2023.130504.

[14] R. Biswas, B. Rai, P. Samui, and S. S. Roy, "Estimating concrete compressive strength using MARS, LSSVM and GP," *Engineering Journal*, vol. 24, no. 2, pp. 41–52, Mar. 2020, doi: 10.4186/ej.2020.24.2.41.

[15] C. Junpradub and K. Asawarungsaengkul, "Predicting the product classification of hot rolled steel sheets using machine learning algorithms," *Engineering Journal*, vol. 27, no. 8, pp. 51–61, Aug. 2023, doi: 10.4186/ej.2023.27.8.51.

[16] S. Wongkamphu and N. Phumchusri, "Hybrid approaches to machine learning for improved battery sales forecasting: A case study in Thailand," *Engineering Journal*, vol. 29, no. 2, pp. 27–43, Feb. 2025, doi: 10.4186/ej.2025.29.2.27.

[17] W. Cheevachaipimol, B. Teinwan, and P. Chutima, "Flight delay prediction using a hybrid deep learning method," *Engineering Journal*, vol. 25, no. 8, pp. 99–112, Aug. 2021, doi: 10.4186/ej.2021.25.8.99.

[18] A. Roshan and M. Abdelrahman, "Improving aggregate abrasion resistance prediction via micro–deval test using ensemble machine learning techniques," *Engineering Journal*, vol. 28, no. 3, pp. 15–24, Mar. 2024, doi: 10.4186/ej.2024.28.3.15.

[19] V. Truong and H. Pham, "Support vector machine for regression of ultimate strength of trusses: A comparative study," *Engineering Journal*, vol. 25, no. 7, pp. 157–166, Jul. 2021, doi: 10.4186/ej.2021.25.7.157.

[20] P. Pintusorachai, W. Tanapalungkorn, and S. Likitlersuang, "Enhancing 3D geological and geotechnical engineering model of Bangkok subsoil using optimal deep neural network models," *Environ. Earth Sci.*, vol. 83, no. 644, pp. 1–19, 2024, doi: 10.1007/s12665-024-11942-2.

[21] W.M. Ridwan, M. Sapitang, A. Aziz, K. F. Kushiar, A. N. Ahmed, and A. El–Shafie, "Rainfall forecasting model using machine learning methods: Case study Terengganu, Malaysia," *Ain Shams Eng. J.*, vol. 12, pp. 1651–1663, 2021, doi: 10.1016/j.asej.2020.09.011.

[22] Y. Yang and T. F. M. Chui, "Reliability assessment of machine learning models in hydrological predictions through metamorphic testing," *Water Resour. Res.*, vol. 57, p. e2020WR029471, 2021, doi: 10.1029/2020WR029471.

[23] A.N. Ahmed, A. Yafouz, A.H. Birima, O. Kisi, Y.F. Huang, M. Sherif, A. Sefelnasr, and A. El–Shafie, "Water level prediction using various machine learning algorithms: a case study of Durian Tunggal river, Malaysia," *Eng. Appl. Comput. Fluid Mech.*, vol. 16, no. 1, pp. 422–440, 2021, doi: 10.1080/19942060.2021.2019128.

[24] S. Zhu, H. Lu, M. Ptak, J. Dai, and Q. Ji, "Lake water–level fluctuation forecasting using machine learning models: A systematic review," *Environ. Sci. Pollut. Control Ser.*, vol. 27, no. 36, pp. 44807–44819, 2020, doi: 10.1007/s11356–020–10917–7.

[25] S. D. Latif and A. N. Ahmed, "Streamflow prediction utilizing deep learning and machine learning algorithms for sustainable water supply management," *Water Resour. Manag.*, vol. 37, no. 8, pp. 3227–3241, 2023, doi: 10.1007/s11269-023-03499-9.

[26] O. Kisi, H. M. Azamathulla, F. Cevat, C. Kulls, M. Kuhdaragh, and M. Fuladipanah, " Enhancing river flow predictions: comparative analysis of machine learning approaches in modeling stage–discharge relationship," *Rineng.*, vol. 22, p. 102017, 2024, doi: 10.1016/j.rineng.2024.102017.

[27] H. Hosseiny, "A deep learning model for predicting river flood depth and extent," *Environ. Model Softw.*,

vol. 145, p. 105186, 2021, doi: 10.1016/j.envsoft.2021.105186.

[28] J. M., Frame, F. Kratzert, D. Klotz, M. Gauch, G. Shalev, O. Gilon, L. M. Qualls, H. V. Gupta, and G. S. Nearing, "Deep learning rainfall–runoff predictions of extreme events," *Hydrol. Earth Syst. Sci.*, vol. 26, pp. 3377–3392, 2022, doi: 10.5194/hess–26–3377–2022.

[29] M. F. Allawi, F. B. Othman, H. A. Afan, A. N. Ahmed, M. S. Hossain, C. M. Fai, and A. El–Shafie, "Reservoir evaporation prediction modeling based on artificial intelligence methods," *Water (Switzerland)*, vol. 11, no. 6, 2019, doi: 10.3390/w11061226.

[30] A. Yafouz, A. N. Ahmed, N. Zaini, and A. El–Shafie, "Ozone concentration forecasting based on artificial intelligence techniques: A systematic review," *Water Air Soil Pollut.*, vol. 232, no. 2, p. 79, 2021, doi: 10.1007/s11270–021–04989–5.

[31] S. Shamshirband, S. Hashemi, H. Salimi, S. Samadianfard, E. Asadi, S. Shadkani, K. Kargar, A. Mosavi, N. Nabipour, and K. W. Chau, "Predicting standardized streamflow index for hydrological drought using machine learning models," *Eng. Appl. Comput. Fluid Mech.*, vol. 14, no. 1, pp. 339–350, 2020, doi: 10.1080/19942060.2020.1715844.

[32] M. Sapitang, W. M. Ridwan, K. F. Kushiar, A. N. Ahmed, and A. El–Shafie, "Machine learning application in reservoir water level forecasting for sustainable hydropower generation strategy," *Sustainability*, vol. 12, no. 15, no. 6121, 2020, doi: 10.3390/su12156121.

[33] I. Ayus, N. Natarajan, and D. Gupta, "Prediction of water level using machine learning and deep learning techniques," *J. Sci. Technol.–Trans. Civ. Eng.*, vol. 2023, pp. 1–12, 2023, doi: 10.1007/s40996–023–01053–6.

[34] A. Osman, H. A. Afan, M. F. Allawi, O. Jaafar, A. Noureldin, F. M. Hamzah, A. N. Ahmed, and A. El–shafie, "Adaptive fast orthogonal search (FOS) algorithm for forecasting streamflow," *J. Hydrol.*, vol. 586, p. 124896, 2020, doi: 10.1016/j.jhydrol.2020.124896.

[35] K. En–Nagre, M. Aqnouy, A. Ouarka, S. A. A. Naqvi, I. Bouizrou, J. E. S. El Messari, A. Tariq, W. Soufan, W. Li, and H. El–Askary, "Assessment and prediction of meteorological drought using machine learning algorithms and climate data," *Clim. Risk Manag.*, vol. 45, p. 100630, 2024, doi: 10.1016/j.crm.2024.100630.

[36] J. F. Ruma, M. S. G. Adnan, A. Dewan, and R. M. Rahman, "Particle swarm optimization–based LSTM networks for water level forecasting: A case study on Bangladesh river network," *Rineng.*, vol. 17, p. 100951, 2023, doi: 10.1016/j.rineng.2023.100951.

[37] Y. Aoulmi, N. Marouf, K. Rasouli, and M. Panahi, "Runoff predictions in a semiarid watershed by convolutional neural networks improved with metaheuristic algorithms and forced with reanalysis and climate data," *J. Hydrol. Eng.*, vol. 28, no. 7, p. 04023018, 2023, doi: 10.1061/JHYEFF.HEENG–5920.

[38] A. Amini, M. Dolatshahi, and R. Kerachian, " Real–time rainfall and runoff prediction by integrating BC–MODWT and automatically–tuned DNNs: Comparing different deep learning models," *J. Hydrol.*, vol. 631, p. 130804, 2024, doi: 10.1016/j.jhydrol.2024.130804.

[39] M. Abbasi, H. Dehban, A. Farokhnia, R. Roozbahani, and M. Bahreinimotlagh, "Long–term streamflow prediction using hybrid SVR–ANN based on Bayesian model averaging," *J. Hydrol. Eng.*, vol. 27, no. 11, p. 05022018, 2022, doi: 10.1061/(ASCE)HE.1943–5584.0002218.

[40] L. Bian, X. Qin, C. Zhang, P. Guo, and H. Wu, "Application, interpretability and prediction of machine learning method combined with LSTM and LightGBM–a case study for runoff simulation in an arid area," *J. Hydrol.*, vol. 625, p. 130091, 2023, doi: 10.1016/j.jhydrol.2023.130091.

[41] P. Umamaheswari and V. Ramaswamy, "An integrated framework for rainfall prediction and analysis using a Stacked Heterogeneous Ensemble Model (SHEM)," *Expert Syst. Appl.*, vol. 256, p. 124831, 2024, doi: 10.1016/j.eswa.2024.124831.

[42] M. Francois, "Scales and power in river basin management: the Chao Phraya River in Thailand," *JSTOR.*, vol. 173, no. 4, pp. 358–73, 2007. [Online]. Available: http://www.jstor.org/stable/30130631

[43] P. Polsomboon, P. Ruangrassamee, and A. Sriariyawat, "Near real–time flood forecasting system for the Greater Chao Phraya River Basin," *J. Hydrol.*, vol. 647, 2025, doi: 10.1016/j.jhydrol.2024.132353.

[44] National Aeronautics and Space Administration, "User guide," 2024, [Online]. Available: https://power.larc.nasa.gov/docs/tutorials/data–access–viewer/user–guide/.

[45] T. Chen and C. Guestrin, "XGBoost: A scalable tree boosting system," presented at *the 22nd ACM SIGKDD International Conference on Knowledge Discovery and Data Mining*, Association for Computing Machinery, San Francisco, Aug. 13–17, 2016, pp. 785–794, doi: 10.1145/2939672.2939785.

[46] A. I. Pathan, L. B. M. Sidek, H. B. Basri, M. Y. Hassan, M. I. A. B. Khebir, S. M. B. A. Omar, M. H. M. Khambali, A. M. Torres, and A. N. Ahmed, "Comparative assessment of rainfall–based water level prediction using machine learning (ML) techniques," *Ain Shams Eng. J.*, vol. 15, no. 2024, p. 102854, 2024, doi: 10.1016/j.asej.2024.102854.

[47] M. Rajesh, P. Indranil, and S. Rehana, "Reservoir inflow forecasting based on gradient boosting regressor model–a case study of Bhadra Reservoir, India," presented at *the 18th Annual Meeting of the Asia Oceania Geosciences Society (AOGS 2021)*, Aug. 1–6, 2021, doi: 10.1142/9789811260100_0022.

[48] M. Rajesh, S. Anishka, P. S. Viksit, and S. Arohi, "Improving short–range reservoir inflow forecasts with machine learning model combination," *Water*

Resour. Manag., vol. 37, pp. 75–90, 2023, doi: 10.1007/s11269–022–03356–1.

[49] S. Jan, U. Khan, A. Khalil, A. A. Khan, H.A. Jan, and I. Ullah, "Use of machine learning techniques in predicting inflow in Tarbela reservoir of Upper Indus Basin," *J. Agric. Meteorol.*, vol. 26, no. 4, pp. 501–504, 2024, doi: 10.54386/jam.v26i4.2676.

[50] M. Maharina, T. Paryono, A. Fauzi, J. Indra, S. Sihabudin, M. K. Harahap, and L. T. Rizki, "Machine learning models for predicting flood events using weather data: an evaluation of logistic regression, LightGBM, and XGBoost," *J. Appl. Data Sci.*, vol. 6, no. 1, pp. 496–507, 2025, doi: 10.47738/jads.v6i1.503.

[51] L. Breiman, "Random forests," *Machine Learning*, vol. 45, pp. 5–32, 2001.

[52] H. Ding, "Using random forest for future sea level prediction," *SHE Web of Conference*, vol. 174, p. 03008, 2023, doi: 10/1051/shsconf/292317403008.

[53] L. Schoppa, M. Disse, and S. Bachmair, "Evaluating the performance of random forest for large–scale flood discharge simulation," *J. Hydrol.*, vol. 590, p. 125531, 2020, doi: 10.1016/j.jhydrol.2020.125531.

[54] K. Sudhakar, S. M. Reddy Mallireddy, P. Tallapureddy, S. Vuddanti, B. Katragadda, and S. R. Manda, "Water level prediction using random forest algorithm," presented at the *7th International Conference on Electronics, Communication and Aerospace Technology (ICECA),* Coimbatore, India, Nov. 22–24, 2023, pp. 1586–1589, doi: 10.1109/ICECA58529.2023.10394849.

[55] T. Yang, A. A. Asanjan, E. Welles, X. Gao, S. Sorooshian, and X. Liu, "Developing reservoir monthly inflow forecasts using artificial intelligence and climate phenomenon information," *Water Resour. Res.*, vol. 53, no. 4, pp. 2786–2812, 2017, doi: 10.1002/2017WR020482.

[56] V. Arunachalam and K. Srinivasa Raju, "Daily reservoir inflow prediction using stacking ensemble of machine learning algorithms," *J. Hydroinformatics*, vol. 26, no. 5, pp. 972–997, 2024, doi: 10.2166/hydro.2024.210.

[57] D. Kim, H. Han, W. Wang, and H.S. Kim, "Improvement of deep learning models for river water level prediction using complex network method," *Water*, vol. 14, no. 466, 2022, doi: 10.3390/w14030466.

[58] R. I. Rasel, N. U. Fokhrul Islam, and A. Haroon, "Application of deep neural network for predicting river tide level," presented at *the International Conference on Innovation in Science, Engineering and Technology (ICISET)*, Oct. 27–28, 2018, Chittagong, Bangladesh. doi: 10.1109/ICISET.2018.8745593.

[59] I. Rehamnia and A. Mahdavi–Meymand, "Advancing reservoir water level predictions: Evaluating conventional, ensemble and integrated swarm machine learning approaches," *Water Resour. Manage.*, vol. 2024, pp. 1–16, 2024, doi: 10.1007/s11269–024–03990–x.

[60] D. Vasudela Rayudu and J. Femila Roseline, "Accurate precipitation prediction using deep learning neural network compared with space vector machine," presented at *the 2023 International Conference on Artificial Intelligence and Knowledge Discovery in Concurrent Engineering (ICECONF)*, Chennai, India, Jan. 5–7, 2023, doi: 10.1109/ICECONF57129.2023.10083591.

[61] T. Izumi, M. Miyoshi, and N. Kobayashi, "Runoff analysis using a deep neural network," presented at *the 12th International Conference on Hydroscience & Engineering: Hydro–Science & Engineering for Environmental Resilience*, Tainan, Taiwan, Nov. 6–10, 2016. [Online]. Available: https://hdl.handle.net/20.500.11970/108556.

[62] R. Abdi, A. Rust, and T. S. Hogue, "Development of a multilayer deep neural network model for predicting hourly river water temperature from meteorological data," *Front Environ. Sci.*, vol. 2021, pp. 9–2021, 2021, doi: 10.3389/fenvs.2021.738322.

[63] J. Changklom, P. Lamchuan, and A. Pornprommin, "Salinity forecasting on raw water for water supply in the Chao Phraya River," *Water*, vol. 14, no. 5, p. 741, 2022, doi: 10.3390/w14050741.

[64] W. Thaisiam, K. Yomwilai, and P. Wongchaisuwat, "Utilizing sequential modelling in collaborative method for flood forecasting," *J. Hydrol.*, vol. 636, no. 2024, p. 131290, 2024, doi: 10.1016/j.jhydrol.2024.131290.

[65] W. Thaisiam, W. Saelo, and P. Wongchaisuwat, "Enhancing a multi–step discharge prediction with deep learning and a response time parameter," *Water*, vol. 14, p. 2898, 2022, doi: 10.3390/w14182898.

Wilmat D.S.M. Priyasiri received a B.Sc. in Applied Sciences from Uva Wellassa University, Sri Lanka. He then completed an M.Eng. in Environmental and Water Resources Engineering at Mahidol University, Thailand, under the Faculty of Engineering. Currently, he is a Ph.D. student at Kyoto University, Japan, in the Civil and Earth Resources Engineering Laboratory. His research interests include hydro–climatology and the impact of climate variability on water resources. He explores the application of machine learning techniques in environmental modelling and hydrological prediction for water resource management.

Areeya Rittima received her doctoral degree in Irrigation Engineering from Kasetsart University, Thailand in 2006. She is currently an associate professor at the Department of Civil and Environmental Engineering, Faculty of Engineering, Mahidol University, Thailand. Her research interests include applications of Artificial Intelligence (AI) for dam–reservoir operation, hydrological prediction, reservoir optimization.

Jidapa Kraisangka received the Ph.D. in Information Science from the University of Pittsburgh, USA in 2019. Currently, she is an assistant professor at the Faculty of Information and Communication Technology, Mahidol University, Thailand. Her research interests are probabilistic and decision–theoretic methods in decision support systems, clinical decision support system machine learning, and data visualization.

Wudhichart Sawangphol received the Master of Information Technology (MIT) with honors in Data Management, Software Engineering, and Knowledge Engineering and Ph.D. in Ontology Reasoning and Optimization from Monash University, Australia in 2013 and 2017. Currently, he is a lecturer at the Faculty of Information and Communication Technology, Mahidol University, Thailand. His research interests are automated reasoning, ontology, ontology reasoning, optimization, machine learning, deep learning, and data visualization.

Yutthana Phankamolsil received the doctoral degree in Irrigation Engineering from Kasetsart University, Thailand in 2008. Currently, he is an assistant professor in the Environmental and Disaster Management Program, Kanchanaburi Campus, Mahidol University, Thailand. His research interests are hydro–informatic, socio–hydrology, agent–based modeling, and micro–irrigation control.

Yutthana Talaluxmana received his doctoral degree in Irrigation Engineering from Kasetsart University, Thailand in 2013. Currently, he is an assistant professor at the Department of Water Resources Engineering, Faculty of Engineering, Kasetsart University, Thailand. His research interests include water resources planning and management, hydraulics engineering, and water resources management.